ORGANIC CHEMISTRY FRONTIERS

RESEARCH ARTICLE

View Article Online
View Journal | View Issue

Cite this: *Org. Chem. Front.*, 2022, **9**, 6295

Synthesis, structure–property relationships and absorbance modulation of highly asymmetric photochromes with variable oxidation and substitution patterns†

Kakishi Uno,‡[a] Dojin Kim, ‡[a] Jonas Bucevicius, [b] Mariano L. Bossi,*[c] Vladimir N. Belov *[a] and Stefan W. Hell[a,c]

Received 5th September 2022,
Accepted 3rd October 2022

DOI: 10.1039/d2qo01399a

rsc.li/frontiers-organic

Asymmetric diarylethenes with benzo[*b*]thiophen-3-yl and 2-thienyl residues having variable oxidation degrees (S and/or SO_2) remained unexplored. These photochromes provide reversibly photoswitchable absorbance and multicolor emission modulation. Here we report 18 photochromic 1,2-diarylperfluorocyclopentenes with oxidized and non-oxidized 2-methylbenzo[*b*]thiophen-3-yl, as well as 5-aryl-3-methylthiophen-2-yl groups. The structure–property relationships were studied for three groups of compounds: non-oxidized, mono-oxidized (to SO_2 in the benzothiophene part), and fully-oxidized (to 2 × SO_2). The quantum chemistry calculations helped to interpret the substituents' effects in each group and predict the photophysical properties of yet unavailable photochromes. The photochromic systems with absorbance modulation introduced in this work were designed for the use in diffraction-unlimited writing and reading with light, nanopattering and optical lithography.

Introduction

Photochromism is the ability of a compound to reversibly switch between two molecular states upon irradiation with light.[1] In most cases, the two states represent isomeric structures, and new chemical bonds are formed and broken intramolecularly in the course of a photochromic reaction. Illumination with light of two distinct wavelengths is required for interconversion (Scheme 1), and the colour change arises from differences in the absorption spectra of the two states (isomers).[2] Diarylethenes[3–5] having benzo[*b*]thiophen-3-yl or 3-thienyl residues attached to the double bond of perfluorocyclopentene,[6] are promising candidates for practical applications. These photochromes feature high photo-reaction efficiency,[7] strong fatigue resistance (large number of switching cycles),[6,8,9] thermal stability of the states,[10] and well separated absorption spectra of the isomers. Due to their unique properties, diarylethenes became attractive molecular tools in various research fields, from material to life science.[11–18] In particular, some diarylethenes present fluorescence emission only in one isomer,[19–26] enabling the most sensitive readout method.

The photo-physical properties of photochromic compounds are strongly influenced by the core structure. So far, a variety of structural modifications have been reported, such as introduction of aryl or other (functional) groups to C-6 of benzo[*b*]thiophene[27,28] or C-5 of thiophene,[29,30] the replacement of these heteroarenes with other heterocycles (*e.g.*, nitrogen-[31,32] or oxygen-containing ones[33,34]), variation of the alkyl group(s) at the "central" reactive carbon atoms (C-2 and C-2′),[35] and the replacement of perfluorocyclopentene by non-fluorinated 5- or 6-membered rings with double bonds.[6,36,37] The syntheses of

[a]*Department of NanoBiophotonics, Max Planck Institute for Multidisciplinary Sciences (MPI NAT), Am Fassberg 11, 37077 Göttingen, Germany. E-mail: kakishi.uno@mpinat.mpg.de, dojin.kim@mpinat.mpg.de, jonas.bucevicius@mpinat.mpg.de, mariano.bossi@mr.mpg.de, vladimir.belov@mpinat.mpg.de, stefan.hell@mpinat.mpg.de*
[b]*Chromatin Labeling and Imaging group, Department of NanoBiophotonics, MPI NAT, Am Fassberg 11, 37077 Göttingen, Germany*
[c]*Department of Optical Nanoscopy Max Planck Institute for Medical Research (MPI MR), Jahnstrasse 29, 69120 Heidelberg, Germany*

†Electronic supplementary information (ESI) available. See DOI: https://doi.org/10.1039/d2qo01399a

‡Equal contribution.

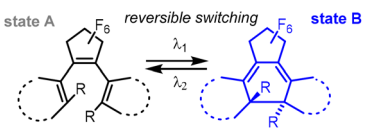

Scheme 1 Under irradiation with light, photochromic 1,2-diarylperfluorocyclopentenes undergo reversible transitions between two stable states.

diarylethenes and their applications in material and life sciences have been studied and reviewed over the last decades.[38–40]

Oxidation of a thiophene/benzo[*b*]thiophene residue to 1,1-dioxide,[41–43] or change from a "normal type" 3-(benzo)thienyl to an "inverse-type" 2-(benzo)thenyl substitution pattern[44–46] are known to drastically alter the conjugation path, optical spectra and the switching parameters of diarylethenes. For example, 1,2-bis(2-alkyl-1-benzothiophene-1,1-dioxide-3-yl)perfluorocyclopentenes[47,48] exhibit high fluorescent quantum yields (up to 0.9) in their closed-form (**CF**).[43] This property makes them useful in many photonic applications: optical memories,[49,50] bioimaging,[51] and super-resolution microscopy.[52,53] On the other hand, the 2-thienyl substituted "inverse type" diarylethenes undergo ring-closure reactions under irradiation in the short wavelength region, and some of them are known to be fluorescent in their open forms (**OFs**).[54] While these chemical modifications are key to customize the photophysical properties, the studies of sulfone (SO_2) and "inverse type" diarylethenes were focused on highly symmetric structures.

Recently, asymmetric "sulfide-sulfone"[55] and "half-inversed sulfone" diarylethenes[56,57] with unique photo-physical properties were reported (Fig. 1, upper part). The former showed ratiometric fluorescence switching (both isomers were fluorescent) and endured more than 2×10^4 switching cycles.[55] The latter switched the emission of an adjacent perylene dye on and off *via* photo-induced electron transfer (PET).[56,57] However, in the previous reports, asymmetric oxidation and "inversed" linkage of the thiophene or benzo[*b*]thiophene units (*via* C-2) were assessed separately, and not combined in one structure. In this work, we used an asymmetric diarylethene, which was applied as a successful modulator in a PET system,[56] as a lead (Fig. 1, DAE-PDI). We varied the substituents (electron donors and acceptors) in both parts (left and right) of the molecule and changed the oxidation state of S-atoms to produce highly asymmetric structures.

In general, the absorption and emission properties of diarylethenes depend on (1) oxidation state of benzo[*b*]thiophene or thiophene core, (2) the presence of donor and/or acceptor groups in the "active" positions of the conjugated system, and (3) the presence and nature of an aryl group at C-6 of benzo[*b*]thiophene. To get insights into the trends of structure–spectra relationships, we designed and prepared 18 photochromic 1,2-diarylperfluorocyclopentenes with 2-methyl-benzo[*b*]thiophen-3-yl and 5-aryl-3-methylthiophen-2-yl parts (Fig. 1, lower part). We categorized them into three groups: non-oxidized (**Ox^0-X-Y**), mono-sulfones (**Ox^1-X-Y** with oxidized benzo[*b*]thiohene units), and bis-sulfones (**Ox^2-X-Y**). In each group, the substituent **X** at the *para*-position of the phenyl group is either hydrogen, or electron-acceptor (**CN**), or electron-donor (**MeO**). In the right part of the molecule, the benzo[*b*]thiophene unit is either non-oxidized or oxidized, and the substituent **Y** = H or phenyl (**Ph**).

Results and discussion

Synthesis

The synthesis routes to the designed 18 compounds and intermediates **A(Y)**, **C(Y)** with variation points **Y** and **Br**, respectively, are shown in Scheme 2. The starting materials, **A(H)** and **A(Ph)** were prepared in 3–4 steps from commercially available materials (see ESI†). The residue **Y** may be hydrogen or any (het)aryl group compatible with the reagents and conditions in Scheme 2. The freshly prepared **A(H)** and **A(Ph)** were reacted with 2-lithio-3-methyl-5-(trimethylsilyl)thiophen to give intermediates **B(H)** and **B(Ph)**, respectively. Treating with bromine in DCM transformed the trimethylsilyl (TMS) group in **B(Y)** to bromides **C(Y)**. The six non-oxidized diarylethenes **Ox^0-X-Y** (see Fig. 1 and Scheme 2) were obtained by a Suzuki–Miyaura reaction of bromides **C(H)** and **C(Ph)** with boronic acids (or esters of boronic acids; see ESI†): *p*-methoxyphenyl, phenyl, and *p*-cyanophenyl. The oxidation of sulfur atoms in both thiophene and benzothiophene fragments to sulfone residues was

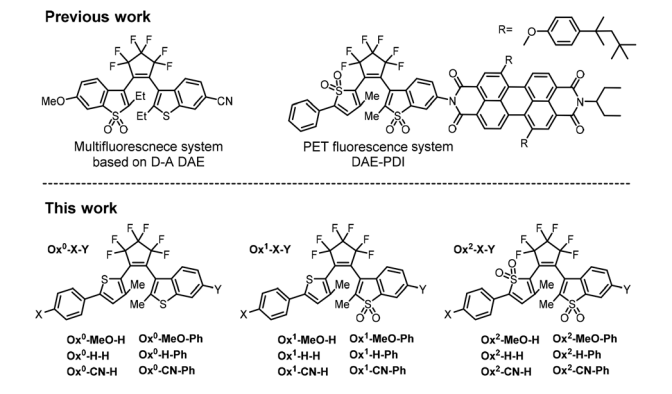

Fig. 1 Upper part: previously reported asymmetric diarylethenes with a sulfone fragment. Lower part: asymmetric structures **Ox^0**, **Ox^1** and **Ox^2** of the present work; **X** and **Y** denote functional groups.

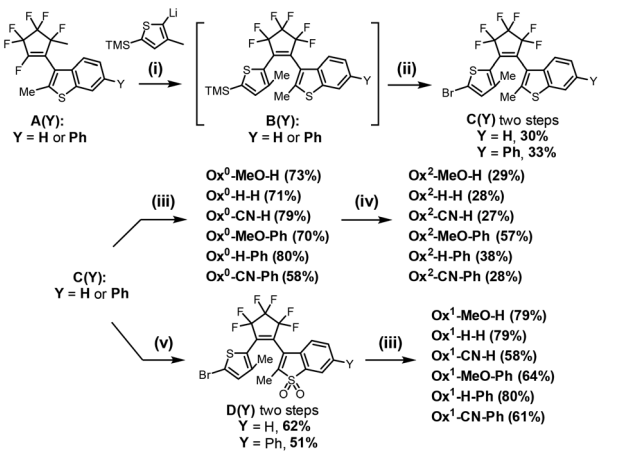

Scheme 2 Synthesis of the diarylethenes: (i) THF, −70 °C; (ii) DCM, Br_2, 0 °C to r.t.; (iii) boronic esters, $Pd(PPh_3)_4$, THF/Na_2CO_3 aq. reflux, 1.5–3.0 h; (iv) *m*CPBA, DCM, r.t., 1–3d; (v) H_2O_2, AcOH, reflux, 30 min.

carried out by treating with excess of *m*-chloroperoxybenzoic acid (*m*CPBA), yielding fully oxidized compounds (**Ox^2-X-Y**). On the other hand, oxidization of compounds **C(Y)** with aqueous H_2O_2 in acetic acid (30 min under reflux) gave sulfones **D(Y)**, in which only benzothiophene units were selectively oxidized. The position of the oxidation site was determined by the comparison of the ^{1}H NMR spectra (characteristic proton shift in the aromatic region), as shown in Fig. S3a and S5a.† Finally, a Suzuki–Miyaura coupling reaction of **D(Y)** with corresponding boronic acids gave asymmetrically oxidized diarylethene series (**Ox^1-X-Y**). The detailed synthetic procedures and NMR spectra (Fig. S1–S23†) of all new compounds are given in ESI.†

Photophysical properties of Ox^0-X-Y and Ox^1-X-Y series

The photoisomerization experiments, measurements of the spectra and photophysical parameters were performed in the home-built optical setup described previously.[58] The photocyclization ($\Phi_{O\rightarrow C}$) and photo-cycloreversion ($\Phi_{C\rightarrow O}$) quantum yields of both series **Ox^0-X-Y** and **Ox^1-X-Y** were determined by using 365 nm and 470 nm light, respectively. The relative fluorescence quantum yields (Φ_F) were determined with quinine sulfate (Φ_F = 0.55 in 0.5 M aq. H_2SO_4), as the reference material. The main photophysical properties of 12 non-oxidized and mono-oxidized diarylethenes are given in Table 1.

In the present study, the photochromic reactions of all asymmetric diarylethenes occurred by irradiation below 560 nm; the "normal" diarylethenes undergo ring-opening reactions at longer wavelengths. For the non-oxidized **Ox^0-X-Y** and mono-sulfone **Ox^1-X-Y** series, the **OF**s showed intense absorption bands in the UV region (320 nm to 420 nm), while the **CF**s' absorption bands appear between 400 nm and 560 nm. Both the cyclization and cycloreversion quantum yields $\Phi_{O\rightarrow C}$ and $\Phi_{C\rightarrow O}$ are high (0.12–0.35). Interestingly, compounds from the **Ox^0-X-Y** and **Ox^1-X-Y** series emit only in their **OF**s, so that their photochromic reactions are accompanied by the reversible "turn-off" type of the fluorescence switch. In other words, upon irradiation with UV light (365 nm), their emission vanishes along with the formation of the **CF**s. Thus, conversions in the photostationary state (PSS) were calculated from the fluorescence modulation (α_{PSS} (365 nm) = IF_{PSS}/IF_0, where IF is the fluorescence intensity at the PSS or before the irradiation, where the entire compound is in the **OF**). Then, the absorption spectrum of the **CF** (Abs_{CF} (λ)) was calculated from the absorption spectra measured of the OF (Abs_{OF} (λ)) and at the PSS (Abs_{PSS} (λ)), according to the following expression Abs_{CF} (λ) = (Abs_{PSS} (λ) − (1 − α_{PSS}) × Abs_{OF} (λ))/α_{PSS}. The irradiation of **CF**s with visible light triggers the ring-opening reactions, with full recovery of the initial fluorescence intensity.

In order to reveal the influence of the substituent **X** (**X** = **CN**, **H**, or **MeO**), the absorption spectra in the series **Ox^0-X-Y** were compared, while **Y** was fixed as **H** (Fig. 2a–c). The group **X** influences the position of the absorption maximum ($_{Abs}\lambda_{max}$) in the **OF**s, but not in the **CF**s. For example, compounds **Ox^0-CN-H**, **Ox^0-H-H**, **Ox^0-MeO-H** in their **OF**s (in 1.4-dioxane) exhibited clear bathochromic shift of the $_{Abs}\lambda_{max}$ values from

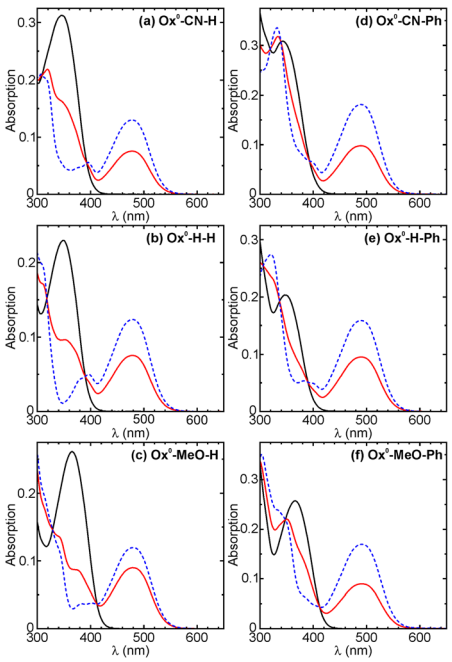

Fig. 2 Absorption spectra of compounds (a) **Ox^0-CN-H**, (b) **Ox^0-H-H**, (c) **Ox^0-MeO-H**, (d) **Ox^0-CN-Ph**, (e) **Ox^0-H-Ph**, and (f) **Ox^0-MeO-Ph** measured in 1,4-dioxane. Black, red and blue (dashed) lines represent the **OF**, the PSS by 365 nm excitation, and the calculated (from emission modulation) **CF** spectra.

Table 1 Photophysical properties of the series **Ox^0-X-Y** and **Ox^1-X-Y** measured in 1,4-dioxane

Compounds	$\Phi_{O\rightarrow C}$ [a]	$\Phi_{C\rightarrow O}$ [b]	$\alpha_{365\ nm}$ [c]	$_{Abs}\lambda_{max}$/nm ($\varepsilon^{OF}\times10^{-3}$) [d]	$_{Abs}\lambda_{max}$/nm ($\varepsilon^{CF}\times10^{-3}$) [e]	$_{Fl}\lambda_{max}$/nm (Φ_F) [f]
Ox^0-H-H/Ox^0-H-Ph	0.18/0.22	0.35/0.33	0.61/0.6	349(15.6)/347(13.5)	480(8.4)/489(10.5)	442 (0.02)/449(0.01)
Ox^1-H-H/Ox^1-H-Ph	0.18/0.14	0.31/0.29	0.77/0.5	363(14.4)/350(16.6)	450(11.2)/463(15.3)	490(0.04)/488(0.05)
Ox^0-MeO-H/Ox^0-MeO-Ph	0.17/0.17	0.33/0.36	0.75/0.53	366(17.4)/366(17.2)	480(8.0)/490(11.3)	472(0.04)/472(0.03)
Ox^1-MeO-H/Ox^1-MeO-Ph	0.12/0.13	0.26/0.36	0.39/0.30	384(15.4)/379(13.2)	452(10.9)/462(12.9)	543(0.09)/534(0.07)
Ox^0-CN-H/Ox^0-CN-Ph	0.15/0.19	0.34/0.41	0.58/0.54	346(20.8)/343(20.6)	478(8.7)/489(12.1)	450(0.02)/467(0.01)
Ox^1-CN-H/Ox^1-CN-Ph	0.20/0.18	0.31/0.30	0.82/0.68	357(18.8)/350(23.1)	446(11.8)/460(16.7)	467(0.04)/469(0.05)

[a] Photo-cyclization quantum yields measured at 365 nm. [b] Photo-cycloreversion quantum yields measured at 470 nm. [c] Photo-conversion degree (α_λ = [CF]/([CF] + [OF])) at the photostationary state by using 365 nm light. [d] Absorption maxima of **OF**s (molar absorptivity; M^{-1} cm^{-1}). [e] Absorption maxima of **CF**s; nm (molar absorptivity; M^{-1} cm^{-1}). [f] Emission maxima; nm (relative fluorescence quantum yields) of **OF**s; standard: quinine sulfate in 0.5M H_2SO_4 (Φ_F = 0.55).[59]

346 nm to 349 nm and 366 nm, respectively; while the $_{Abs}\lambda_{max}$ value of the **CF**s remained almost unchanged (479 nm ± 1 nm, Table 1). The similar trend is observed in the series **Ox^0-X-Ph** and **Ox^1-X-Y** (Y = H, Ph). For detailed comparison, the absorption spectra of compounds **Ox^0-X-Ph** are shown in Fig. 2d–f; see also Table 1. The influence of the substituents **X** and **Y** on the $_{Abs}\lambda_{max}$ values were further assessed by using quantum chemical calculations and compared with the features observed for the double oxidized analogs **Ox^2-X-Y** in the following sections. In what concerns emission intensity, all Φ_F values of **Ox^1-X-Y** in their **OF**s (measured in 1.4-dioxane) are approximately 2–4 times higher than these of **Ox^0-X-Y** (Table 1). The nature of the **Y** substituent attached to benzothiophene (or benzothiophene sulfone) has almost no influence on fluorescence, but the residue **X** influences the Φ_F values and the position of emission maxima ($_{Fl}\lambda_{max}$; see Table 1).

To explore the substituent effects in the **Ox^1-X-Y** series, we considered three compounds **Ox^1-X-H** (**X** = **CN**, **H**, and **MeO**). Their photo-switching and emission in solvents of various polarity (cyclohexane, ethyl acetate, and acetonitrile) were studied. The fluorescence spectra and the photophysical data are given in Fig. 3a–c and Table 2, respectively. We found that both **Ox^1-CN-H** and **Ox^1-H-H** switch reversibly between fluorescent and non-fluorescent states, regardless of the solvent polarity (Fig. 3a and b). These two compounds showed similar emission efficiencies and photoreaction quantum yields ($\Phi_{O\rightarrow C}$ and $\Phi_{C\rightarrow O}$) in all solvents we used. On the other hand, the fluorescent properties of **Ox^1-MeO-H** strongly depends on the solvent polarity. Compared to **Ox^1-CN-H** and **Ox^1-H-H**, the Φ_F value and the photoswitching quantum yields of **Ox^1-MeO-H** were found to be 5 times lower in acetonitrile

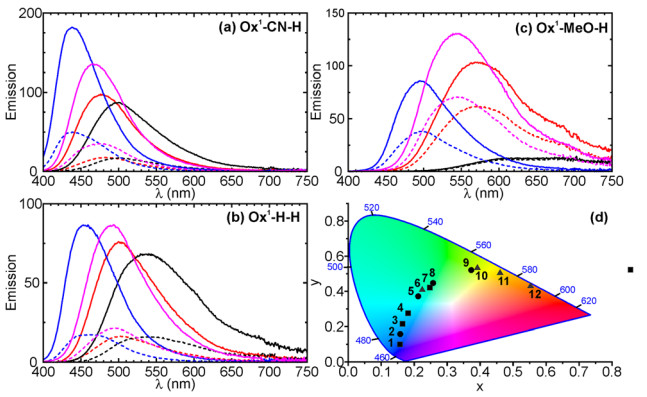

Fig. 3 Emission spectra of (a) **Ox^1-CN-H**, (b) **Ox^1-H-H** and (c) **Ox^1-MeO-H** in the **OF**s (solid lines) and in the photostationary state ($\alpha^{365\ nm}$; dashed lines), in cyclohexane (blue lines), dioxane (purple lines), ethyl acetate (red lines) and acetonitrile (black lines). (d) CIE 1931 color space with emission colors of three compounds, in squares for **Ox^1-CN-H** (*i.e.*, 1, 3, 4, and 7 represent color of **Ox^1-CN-H** in cyclohexane (cHex), dioxane (Diox), ethyl acetate (EtAc), and acetonitrile (MeCN), respectively), circles for **Ox^1-H-H** (2, 5, 8, and 9 represent colors in cHex, Diox, EtAc, and MeCN, respectively) and triangles for **Ox^1-MeO-H** (6, 10, 11, and 12 represent colors in cHex, Diox, EtAc, and MeCN, respectively).

Table 2 Photo-switching and fluorescent properties of **Ox^1-X-Y** in various solvents

	Solvent [a]	$\Phi_{O\rightarrow C}$ [b] ($\Phi_{C\rightarrow O}$)	$\alpha_{(365\ nm)}$ [c]	$_{Fl}\lambda_{max/nm}$(Eff$_F$) [d]
Ox^1-CN-H	cHex	0.13 (0.27)	0.73	438 (1.15)
	Diox	0.20 (0.31)	0.82	467 (1.00)
	EtAc	0.12 (0.23)	0.82	476 (0.78)
	MeCN	0.12(0.20)	0.81	500 (0.81)
Ox^1-H-H	cHex	0.14 (0.28)	0.80	454 (0.84)
	Diox	0.18 (0.31)	0.77	490 (1.00)
	EtAc	0.12 (0.23)	0.78	502 (0.96)
	MeCN	0.11 (0.22)	0.76	537 (1.13)
Ox^1-MeO-H	cHex	0.14 (0.25)	0.56	495 (0.49)
	Diox	0.12 (0.26)	0.39	543 (1.00)
	EtAc	0.08 (0.20)	0.40	572 (0.88)
	MeCN	0.02 (0.24)	0.09	616 (0.13)

[a] cHex, Diox, EtAc, and MeCN are cyclohexane, 1,4-dioxane, ethyl acetate, and acetonitrile respectively. [b] Photo-cyclization and photocycloreversion quantum yields measured by using 365 nm and 470 nm light sources, respectively. [c] The photo-conversion degrees at the photo-stationary state (PSS) by using 365 nm light were calculated from the degrees of the fluorescence quench of **OF**s. [d] The emission maxima (relative emission efficiencies referenced to the value measured in 1,4-dioxane; the absolute values are in Table 1).

(Table 2). It was also found that the emission intensity of **Ox^1-MeO-H** depends on the solvent polarity much stronger than these of **Ox^1-CN-H** and **Ox^1-H-H** (Fig. 3c). The solvatochromism of **Ox^1-MeO-H** is a result of the strong intramolecular charge-transfer (CT) in the excited state of the **OF**, induced by the conjugation between the methoxy (donor) and the benzothiophene sulfone (acceptor) groups. To quantitatively illustrate the solvatochromic fluorescence of compounds **Ox^1-X-H**, their emission maxima are plotted in the CIE 1931 color space diagram as shown in the Fig. 3d.

Photophysical properties of Ox^2-X-Y

Unlike compounds in the series **Ox^0-X-Y** and **Ox^1-X-Y**, the fully oxidized **Ox^2-X-Y** analogs were non-fluorescent both in their **OF**s and **CF**s and exhibited either low photoreaction quantum yields ($\Phi_{O\rightarrow C}$ and $\Phi_{C\rightarrow O}$) or irreversible photoreactions. We found that only **Ox^2-MeO-H** and **Ox^2-MeO-Ph** can undergo reversible photochromic transformations. The unique feature is that these two compounds exhibited "inversed" photochromism: the absorption bands of the **OF**s were found at longer wavelengths than these of the **CF**s. The photochromism of **Ox^2-MeO-H**, **Ox^2-MeO-Ph** and their photophysical parameters are given in Fig. 4 and Table 3, respectively. The absorption bands of the open and closed forms overlapped, and in order to achieve the highest possible photo-conversion degree, the irradiation wavelengths had to be carefully selected. We found that 455 nm and 365 nm light sources are optimal for photocyclization and cycloreversion reactions, respectively. In the case of **Ox^2-MeO-H**, irradiation with 455 nm light of the solution in 1,4-dioxane led to the decrease of the absorption band of the **OF** ($_{Abs}\lambda_{max}$ = 406 nm), while the new absorption band peaking at 355 nm emerged. Then the solution of **Ox^2-MeO-H** was analyzed by means of HPLC and HRMS, and we confirmed that the new absorption band ($_{Abs}\lambda_{max}$ = 355 nm) is due to the

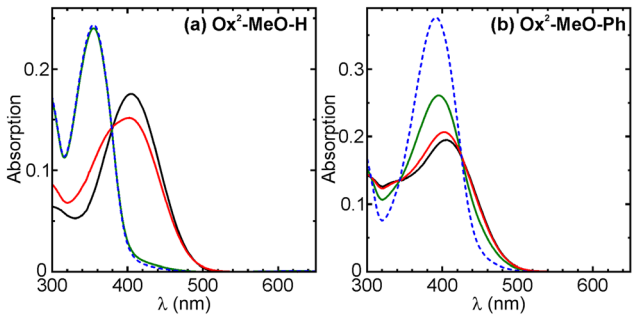

Fig. 4 The absorption spectra of (a) **Ox²-MeO-H** and (b) **Ox²-MeO-Ph**, where black, red, green lines and blue-dashed line correspond to the **OF**s, PSS under irradiation with 365 nm light, PSS under irradiation with 455 nm light, and calculated **CF**s, respectively.

Table 3 The key photophysical data of **Ox²-MeO-H** and **Ox²-MeO-Ph**

	$\Phi_{O\rightarrow C}$ [a]	$\Phi_{C\rightarrow O}$ [b]	$\alpha_{(455\ nm)}$ [c]	$\alpha'_{(365\ nm)}$ [d]
Ox²-MeO-H	9.7×10^{-3}	1.3×10^{-2}	0.98	0.81
Ox²-MeO-Ph	1.1×10^{-2}	6.4×10^{-2}	0.39	0.91

[a] Photo-cyclization quantum yields measured with 455 nm light. [b] Photo-cycloreversion quantum yields measured with 365 nm light. [c] The photo-conversion degrees at the photostationary states (PSS) by using 455 nm light (α_λ = [CF]/([CF] + [OF])) was measured by HPLC. [d] The photo-conversion degrees at the photostationary states (PSS) by using 365 nm light (α'_λ = [OF]/([CF] + [OF])) was measured by HPLC.

formation of the **CF** of **Ox²-MeO-H** (Fig. 4a). Moreover, HPLC analysis revealed that the photo-conversion by 455 nm light is almost quantitative ($\alpha_{(455nm)} > 0.98$), due to the well-separated absorption bands between **OF** and **CF** of **Ox²-MeO-H** (*i.e.* **CF** has almost no absorption at 455 nm). As a control, when 405 nm light was employed, the conversion became incomplete ($\alpha^{405\ nm} = 0.74$). Further irradiation with 365 nm light regenerated the **OF** (Fig. 4a), and the reverse photo-conversion degree ($\alpha'_{(365nm)} = 1 - \alpha_{(365nm)}$ = [OF]/([CF] + [OF])) was determined to be 0.81 by HPLC analysis. The enhancement in the absorbance at 355 nm achieved between the two photo-stationary states is ×2.2. The photophysical properties of **Ox²-MeO-Ph** were also studied under the same irradiation condition. In comparison to **Ox²-MeO-H**, a lower photo-conversion degree to the **CF** was observed ($\alpha^{455\ nm} = 0.39$). This is a result of a smaller shift in the absorption maxima between the **OF** and the **CF**, *i.e.* due to considerable absorption of the **CF** at 455 nm (Fig. 4b). The phenyl substituent (**Y**) attached to benzothiophene sulfone induced the bathochromic shift of the **CF**'s absorption band, resulting in a larger overlap with the absorption band of the **OF**. From the measurements of the whole **Ox²-X-Y** series, we found that introduction of an electron donating (*e.g.*, methoxy) group (as **X**) and the absence of aryl groups at C-6 of the oxidized benzothiophene part, are key factors in the design of the "inverse type" photochromic diarylethenes. The factors reduce the undesired overlap of the absorption bands of the **OF** and **CF**.

Quantum chemical calculations

To gain a better understanding of the structure–property relationships of the new asymmetric photochromes, we performed the density functional theory (DFT) calculations by using Gaussian 09 program package.[60] The geometries of compounds were optimized using B3LYP exchange–correlation hybrid functional together with the 6-31++G(d,p) basis set in vacuum of both **OF**s (*anti-parallel* conformer) and **CF**s (*anti-parallel* conformer). We have calculated energies and obtained the isodensity surface plots of the frontier molecular orbitals (FMO). In the series of **CF**s of **Ox⁰-X-Y**, both HOMO and LUMO are localized on the whole molecule excluding substituent **X** and the neighbouring phenyl ring (Fig. 5a). This results in closely similar energy values of the HOMO–LUMO gaps for the whole series. In the case where **Y** = phenyl, the localization of FMO's is extended on this phenyl ring (attached to the benzothiophene), but does not involve the phenyl substituent attached to the thiophene ring (Fig. 5a). Usually, the lowest energy transition from the ground state is between HOMO and LUMO. This nicely explains, why substituent **X** does not affect the absorption maxima of the **CF** and why switching from **Y** = H to **Y** = Ph results in a bathochromic shift. In the **OF**s of **Ox⁰-X-Y** series, HOMO is localized on all molecular π-system, including the phenyl substituent; it also applies, if **Y** = Ph (Fig. 5b). Yet, the LUMO localization partially excludes the benzothiophene residue and the substituent **Y**, which explains the observation that the absorption maxima of **OF**s are mainly affected by substituent **X** but not **Y**. Similar regularities are also valid for the **Ox¹-X-Y** series of compounds (Fig. S24†).

The localization of FMOs in the series **Ox²-X-Y** indicates a strong charge transfer character of the excited state and was not sufficient to explain the demonstrated "inversed photochromism" of **Ox²-MeO-H(Ph)** compounds (Fig. S24–S28†). In order to get better understanding of the nature of the absorption bands, we included 1,4-dioxane as solvent with IEFPCM solvation model and calculated the vertical excitation energies based on TD-DFT with CAM-B3LYP/6-31++G(d,p) hybrid exchange–correlation functional. The latter includes the long-range corrections and performs well with charge transfer transitions. The significant similarity between experimental and theoretical absorption spectra were observed (Fig. 5c and d). For the **CF** of **Ox²-MeO-H**, the lowest energy transition $S_0 \rightarrow S_1$ is not a usual HOMO–LUMO transition (which becomes forbidden, due to a significantly small orbital overlap), but it is a HOMO−1 → LUMO transition instead. This results in a higher energy difference, and therefore, the absorption band of the **CF** is observed at the unusually short wavelengths (Fig. 5c). In the **OF** of **Ox²-MeO-H**, the $S_0 \rightarrow S_1$ excitation arises from a mix of HOMO → LUMO and HOMO-3 → LUMO events. For the **CF** of **Ox²-MeO-Ph**, the $S_0 \rightarrow S_1$ transition involves similar type of mixed orbitals (Fig. 5d). The lowest energy band of the **CF** of **Ox²-MeO-Ph** again excluded the HOMO orbital and relied on a mixed (HOMO−1 + HOMO-4) to LUMO transition. We hypothesize that the exclusion of HOMO in the series of **Ox²-MeO-Y (OFs)** is due to a spatially very small overlap of FMO's at the sulfone oxygen atoms (Fig. S24–S28†), which forbids a HOMO

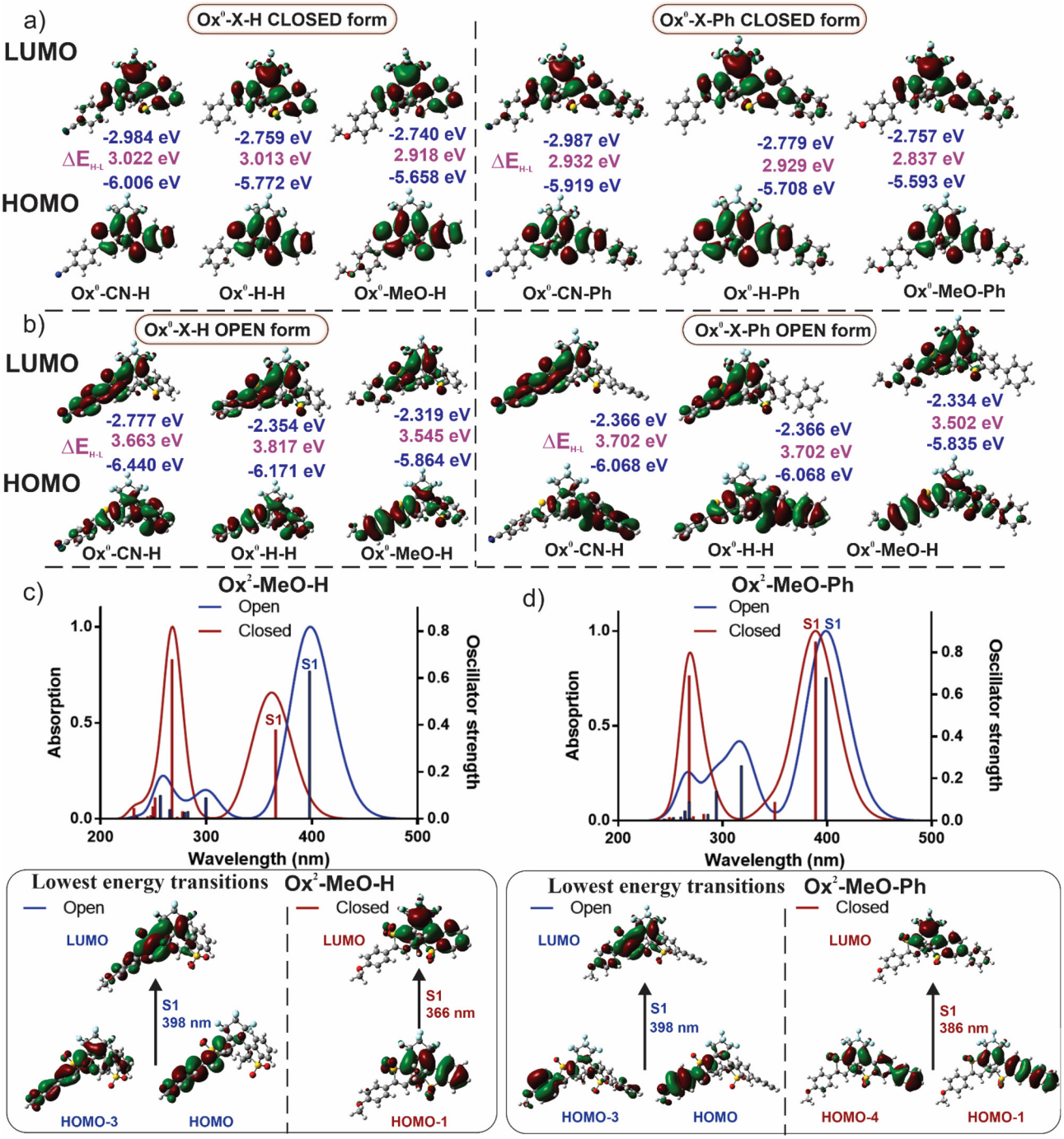

Fig. 5 The DFT calculated ground state isodensity surface plots of the FMOs in (a) **CF**s and (b) **OF**s of **OX^0-X-Y** series. TD-DFT simulated vertical excitation energies including 1,4-dioxane as solvent with IEFPCM model and fitted absorption spectra on excitation bands and representation of molecular orbitals responsible for the lowest energy transitions for (c) **Ox^2-MeO-H** and (d) **Ox^2-MeO-Ph** in **OF**s and **CF**s.

→ LUMO transition and results in inversed absorption bands of **CF**s and **OF**s. The calculations reasonably predicted the positions and trends in the experimentally observed lowest energy absorption bands, including rapprochement of the **CF** and **OF** of **Ox^2-MeO-Ph**; thus giving a better insight into the nature and control of "inverse photochromism" (Fig. 5 and S25–S28†). The experimental data and quantum chemical calculations introduced in this paper will serve for the design and optimization of "inversed" diarylethene photoswhitches with well-separated bands of the **OF** and **CF**.

Absorbance modulation

As easily processable substances, organic photoswitchable dyes are of high interest for new optical recording systems. In

the far-field photolithography, the optical resolution is limited by diffraction to a half of the wavelength of the irradiation source.[61] The reversible optical switching between two stable molecular states was recognized as a new physical concept enabling to "break the diffraction barrier" and applicable in lens-based optical imaging, as well as writing at the nanoscale.[62] Improving the optical resolution in recording media through the use of photochromic layers was mainly developed by Rajesh Menon under the name "Absorbance Modulation Optical Lithography (AMOL)".[63] The photochromic dyes are appealing as main materials for writing at the nanoscale, because they feature transitions between two stable ground states (Scheme 1). Thus, light of low intensities may be applied.[62] It preserves the photochromic layer from degradation, and the performance (contrast ratio and optical resolution) of the recording system is improved. Unfortunately, none of the photochromic diarylethenes reported so far possesses the absorption modulation properties required for the lens-based writing at the nanoscale: strong change of absorption at the certain wavelength, high degree of conversion in a photostationary state, photostability (high number of switching cycles), and the controllable switching kinetics. The symmetric diarylethene based on the two 5,5′-dimethyl-2,2′-bithiophene units attached *via* positions 4 to the double bond (C-1 and C-2) of the perfluorocyclopentane bridge has been reported as benchmark material for AMOL.[63] It requires the use of 325 nm light for performing the ring-closure reaction. The ring-opening step (irradiation at 633 nm) is very slow, with quantum efficiency *ca.* 10^{-5}–10^{-6}, and this reduces the number of achievable switching cycles. Surprisingly, other diarylethenes have not yet been applied in AMOL.[63,64] Therefore, one of our goals was to offer a general synthetic route to photochromic diarylethenes capable of efficient and rapid absorbance modulation with focusable light.

The aberration corrected lenses with large numerical apertures (1.35–1.45) are available only for wavelengths greater than 360 nm. In line with this, compact and affordable diode lasers emitting at 375 nm provide one of the shortest wavelengths available for optical switching and lens-based writing at the nanoscale. As an example, in Fig. 6 we present the absorption modulation of compound **Ox^0-MeO-H** dissolved in 1,4-dioxane. Table 1 contains the data on photophysical properties. The absorption modulation at 375 nm is about 2.5 fold. In other organic solvents (ethyl acetate, acetonitrile and cyclohexane), similar properties were observed. These organic solvents are compatible with polymer matrixes in which the photochromic compounds are applied for nanolithography.

For compound in Fig. 6, the degree of conversion in the photostationary state (transition to the closed-ring isomer in Scheme 1) is relatively high (75% under irradiation with 365 nm light), but the cyclization is not complete. However, incomplete conversion does not preclude secure writing based just on discerning between exposed and non-exposed areas. In AMOL, a thin film of photochromic material is placed on top of a conventional photoresist and illuminated simultaneously by a focused light of wavelength λ_1 and another irradiation

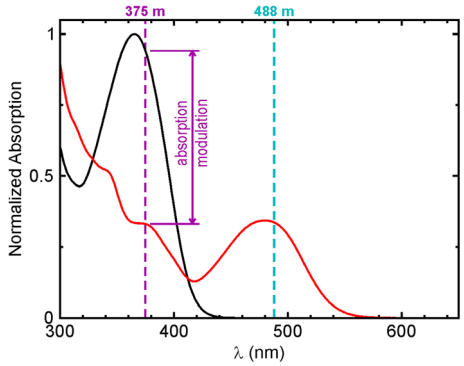

Fig. 6 Absorption modulation of compound **Ox^0-MeO-H** in 1,4-dioxane solution; for structure, see Fig. 1; for photophysical properties, see Table 1.

pattern of wavelength λ_2 featuring the local minimum or minima (*e.g.*, a doughnut-shaped beam).[62–65] The λ_1 beam transforms the photochromic material to a more transparent (at λ_1) state, and the underlying photoresist may be exposed. However, the λ_2 irradiation reverses the transformation in all areas, except the local minimum (minima), so that the photoresist remains exposed only in these subdiffractionally "squeezed" areas. As a result, higher photolithographic resolution and information density may be achieved. This is expected to be the case for compound **Ox^0-MeO-H** (Fig. 6), as well as diarylethenes **Ox^1-CN-H** and **Ox^0-CN-Ph** (Table 1), if we apply 375 nm and 488 nm lasers as λ_1 and λ_2 irradiation sources, respectively. The main advantages over the benchmark compound[63] are that the use of 325 nm light is avoided, and the cycloreversion quantum yield increased over several orders of magnitude. We consider the structure–spectra relationships found in the series of asymmetric diarylethenes with variable oxidation patterns as guidelines for the design of absorbance modulators applicable for writing and reading on nanoscale with visible light.

Conclusions

In this work, the structure–properties relationships of highly asymmetric photochromic diaryethenes were studied. Eighteen new compounds were designed, and their syntheses performed. The three groups – non-oxidized **Ox^0-X-Y**, mono-oxidized **Ox^1-X-Y**, and fully-oxidized **Ox^2-X-Y** – were compared, in which the substituents **X** = **CN**, **H**, or **MeO** and **Y** = **H** or **Ph**. It was found that the **OF**s of **Ox^0-X-Y** and **Ox^1-X-Y** are weakly fluorescent. Among them, compound **Ox^1-MeO-H** with an electron donating methoxy group showed the highest value of Φ_F and the strongest solvatochromism (in respect of emission color), due to the CT effect in the excited state. Interestingly, the fully oxidized diarylethene reported by Fukaminato *et al.*[56] also showed reverse-type photochromism. However, this phenomenon is rare. In the present study, only **Ox^2-MeO-H** and **Ox^2-MeO-Ph** having methoxy groups underwent the reverse-type

photochromic reaction. Our study revealed that the absorption bands of **OF** and **CF** of **Ox^2-MeO-H** are fully separated, enabling the full conversion to **CF** by irradiation of 455 nm. We explained the observed substituents' effect and the nature of inverse photochromism by using DFT calculations. We found that the large hypsochromic shifts observed in **CF**s of **Ox^2-MeO-H** and **Ox^2-MeO-Ph** are ascribed to the "forbidden" and hybrid HOMO–LUMO transitions.

We believe that the findings reported here will contribute to the development of photochromic compounds applicable as highly efficient molecular switches in material and life sciences. We plan to design and test the photoswitching performance of absorbance modulators in organic solvents and polymer matrices.

Conflicts of interest

There are no conflicts to declare.

Acknowledgements

We thank J. Bienert (MPI NAT), Dr H. Frauendorf, and Dr M. John and co-workers (Institut für Organische und Biomolekulare Chemie, Georg-August-Universitat, Göttingen, Germany) for recording NMR and high resolution mass spectra. Open Access funding provided by the Max Planck Society.

References

1 H. Bouas-Laurent and H. Dürr, Organic photochromism (IUPAC Technical Report), *Pure Appl. Chem.*, 2001, **73**, 639–665.
2 K. Nakatani, J. Piard, P. Yu and R. Métivier, *Photochromic Materials*, ed. H. Tian and J. Zhang, Wiley, Weinheim, 2016, pp. 1–45.
3 M. Irie, Y. Yokoyama and T. Seki, *New Frontiers in Photochromism*, Springer, Tokyo, 2013, pp. 3–116.
4 H. Tian and S. Yang, Recent progresses on diarylethene based photochromic switches, *Chem. Soc. Rev.*, 2004, **33**, 85–97.
5 M. Irie, T. Fukaminato, K. Matsuda and S. Kobatake, Photochromism of Diarylethene Molecules and Crystals: Memories, Switches, and Actuators, *Chem. Rev.*, 2014, **114**, 12174–12277.
6 M. Hanazawa, R. Sumiya, Y. Horikawa and M. Irie, Thermally irreversible photochromic systems. Reversible photocyclization of 1,2-bis (2-methylbenzo[*b*]thiophen-3-yl) perfluorocyclocoalkene derivatives, *J. Chem. Soc., Chem. Commun.*, 1992, 206–207.
7 S. Fukumoto, T. Nakashima and T. Kawai, Photon-Quantitative Reaction of a Dithiazolylarylene in Solution, *Angew. Chem., Int. Ed.*, 2011, **50**, 1565–1568.
8 Y.-C. Jeong, D. G. Park, E. Kim, K.-H. Ahn and S. I. Yang, Fatigue-resistant photochromic dithienylethenes by controlling the oxidation state, *Chem. Commun.*, 2006, 1881–1883.
9 M. Herder, B. M. Schmidt, L. Grubert, M. Pätzel, J. Schwarz and S. Hecht, Improving the Fatigue Resistance of Diarylethene Switches, *J. Am. Chem. Soc.*, 2015, **137**, 2738–2747.
10 M. Irie, T. Lifka, S. Kobatake and N. Kato, Photochromism of 1,2-Bis(2-methyl-5-phenyl-3-thienyl)perfluorocyclopentene in a Single-Crystalline Phase, *J. Am. Chem. Soc.*, 2000, **122**, 4871–4876.
11 K. Higashiguchi, G. Taira, J. Kitai, T. Hirose and K. Matsuda, Photoinduced Macroscopic Morphological Transformation of an Amphiphilic Diarylethene Assembly: Reversible Dynamic Motion, *J. Am. Chem. Soc.*, 2015, **137**, 2722–2729.
12 J. Okuda, Y. Tanaka, R. Kodama, K. Sumaru, K. Morishita, T. Kanamori, S. Yamazoe, K. Hyodo, S. Yamazaki, T. Miyatake, S. Yokojima, S. Nakamura and K. Uchida, Photoinduced cytotoxicity of a photochromic diarylethene via caspase cascade activation, *Chem. Commun.*, 2015, **51**, 10957–10960.
13 H. Sato, T. Matsui, Z. Chen, J. Pirillo, Y. Hijikata and T. Aida, Photochemically Crushable and Regenerative Metal–Organic Framework, *J. Am. Chem. Soc.*, 2020, **142**, 14069–14073.
14 T. Fukushima, K. Tamaki, A. Isobe, T. Hirose, N. Shimizu, H. Takagi, R. Haruki, S. Adachi, M. J. Hollamby and S. Yagai, Diarylethene-Powered Light-Induced Folding of Supramolecular Polymers, *J. Am. Chem. Soc.*, 2021, **143**, 5845–5854.
15 F. Terao, M. Morimoto and M. Irie, Light-Driven Molecular-Crystal Actuators: Rapid and Reversible Bending of Rodlike Mixed Crystals of Diarylethene Derivatives, *Angew. Chem., Int. Ed.*, 2012, **51**, 901–904.
16 R. Nishimura, K. Hyodo, H. Sawaguchi, Y. Yamamoto, Y. Nonomura, H. Mayama, S. Yokojima, S. Nakamura and K. Uchida, Fractal Surfaces of Molecular Crystals Mimicking Lotus Leaf with Phototunable Double Roughness Structures, *J. Am. Chem. Soc.*, 2016, **138**, 10299–10303.
17 M. Berberich, A.-M. Krause, M. Orlandi, F. Scandola and F. Würthner, Toward Fluorescent Memories with Nondestructive Readout: Photoswitching of Fluorescence by Intramolecular Electron Transfer in a Diaryl Ethene-Perylene Bisimide Photochromic System, *Angew. Chem., Int. Ed.*, 2008, **47**, 6616–6619.
18 M. Berberich and F. Würthner, Terrylene bisimide-diarylethene photochromic switch, *Chem. Sci.*, 2012, **3**, 2771–2777.
19 G. Naren, S. Li and J. Andréasson, A simplicity-guided cocktail approach toward multicolor fluorescent systems, *Chem. Commun.*, 2020, **56**, 3377–3380.
20 M. Takeshita and M. Irie, Reversible Fluorescence Intensity Change of a Diarylethene, *Chem. Lett.*, 1998, 1123.

21 K. Yagi and M. Irie, Fluorescence Property of Photochromic Diarylethenes with Indole Groups, *Bull. Chem. Soc. Jpn.*, 2003, **76**, 1625.
22 F. Hu, L. Jiang, M. Cao, Z. Xu, J. Huang, D. Wu, W. Yang, S. H. Liu and J. Yin, Cyanine-based dithienylethenes: synthesis, characterization, photochromism and biological imaging in living cells, *RSC Adv.*, 2015, **5**, 5982–5987.
23 H. Liu and Y. Chen, The Photochromism and Fluorescence of Diarylethenes with a Imidazole Bridge Unit: A Strategy for the Design of Turn-on Fluorescent Diarylethene System, *J. Phys. Chem. A*, 2009, **113**, 5550–5553.
24 S. C. Pang, H. Hyun, S. Lee, D. Jang, M. J. Lee, S. H. Kang and K. H. Ahn, Photoswitchable fluorescent diarylethene in a turn-on mode for live cell imaging, *Chem. Commun.*, 2012, **48**, 3745–3747.
25 T. Nakagawa, Y. Miyasaka and Y. Yokoyama, Photochromism of a spiro-functionalized diarylethene derivative: multi-colour fluorescence modulation with a photon-quantitative photocyclization reactivity, *Chem. Commun.*, 2018, **54**, 3207–3210.
26 Z. Xu, Q. T. Liu, X. Wang, Q. Liu, D. Hean, K. C. Chou and M. O. Wolf, Quinoline-containing diarylethenes: bridging between turn-on fluorescence, RGB switching and room temperature phosphorescence, *Chem. Sci.*, 2020, **11**, 2729–2734.
27 K. Matsuda and M. Irie, Photochromism of Diarylethenes with Two Nitronyl Nitroxides: Photoswitching of an Intramolecular Magnetic Interaction, *Chem. – Eur. J.*, 2001, **7**, 3466–3473.
28 J. Lee, T. Kwon and E. Kim, Electropolymerization of an EDOT-modified diarylethene, *Tetrahedron Lett.*, 2007, **48**, 249.
29 M. Bossi, V. Belov, S. Polyakova and S. W. Hell, Reversible Red Fluorescent Molecular Switches, *Angew. Chem., Int. Ed.*, 2006, **45**, 7462–7465.
30 F. Hu, M. Cao, X. Ma, S. H. Liu and J. Yin, Visible-Light-Dependent Photocyclization: Design, Synthesis, and Properties of a Cyanine-Based Dithienylethene, *J. Org. Chem.*, 2015, **80**, 7830–7835.
31 H. B. Cheng, Y. D. Huang, L. Zhao, X. Li and H. C. Wu, A prominent bathochromic shift effect of indole-containing diarylethene derivatives, *Org. Biomol. Chem.*, 2015, **13**, 3470–3475.
32 F. Ortica, P. Smimmo, U. Mazzucato, G. Favaro, A. Heynderickx, C. Moustrou and A. Samat, Photoinduced Processes in Dipyrrolyl-Perfluoro-Cyclopentenes, *Photochem. Photobiol.*, 2006, **82**, 1326–1333.
33 T. Yamaguchi, W. Taniguchi, T. Ozeki, S. Irie and M. Irie, Photochromism of diarylethene oxazole derivatives in a single-crystalline phase, *J. Photochem. Photobiol., A*, 2009, **207**, 282.
34 S. Pu, H. Li, G. Liu, W. Liu, S. Cui and C. Fan, Synthesis and the effects of substitution upon photochromic diarylethenes bearing an isoxazole moiety, *Tetrahedron*, 2011, **67**, 1438–1447.
35 T. Yamaguchi and M. Irie, Photochromism of bis(2-alkyl-1-benzothiophen-3-yl)perfluorocyclopentene derivatives, *J. Photochem. Photobiol., A*, 2006, **178**, 162.
36 S. Chen, Y. Yang, Y. Wu, H. Tian and W. Zhu, Multi-addressable photochromic terarylene containing benzo[*b*]thiophene-1,1-dioxide unit as ethene bridge: multifunctional molecular logic gates on unimolecular platform, *J. Mater. Chem.*, 2012, **22**, 5486–5494.
37 D. Kitagawa, T. Nakahama, Y. Nakai and S. Kobatake, 1,2-Diarylbenzene as fast T-type photochromic switch, *J. Mater. Chem. C*, 2019, **7**, 2865–2870.
38 J. Zhang and H. Tian, The Endeavor of Diarylethenes: New Structures, High Performance, and Bright Future, *Adv. Opt. Mater.*, 2018, **6**, 1701278.
39 K. Uno, V. N. Belov and M. L. Bossi, Photoswitchable Fluorophores for Super-Resolution Optical Microscopy, in *Molecular Photoswitches*, ed. Z. L. Pianowski, Wiley VCH, 2022, vol. 2, pp. 605–626.
40 D. Kim and S. Y. Park, Multicolor Fluorescence Photoswitching: Color-Correlated versus Color-Specific Switching, *Adv. Opt. Mater.*, 2018, **6**, 1800678.
41 Y.-C. Jeong, S. I. Yang, K.-H. Ahn and E. Kim, Highly fluorescent photochromic diarylethene in the closed-ring form, *Chem. Commun.*, 2005, 2503–2505.
42 M. Taguchi, T. Nakagawa, T. Nakashima and T. Kawai, Photochromic and fluorescence switching properties of oxidized triangle terarylenes in solution and in amorphous solid states, *J. Mater. Chem.*, 2011, **21**, 17425–17432.
43 K. Uno, H. Niikura, M. Morimoto, Y. Ishibashi, H. Miyasaka and M. Irie, In Situ Preparation of Highly Fluorescent Dyes upon Photoirradiation, *J. Am. Chem. Soc.*, 2011, **133**, 13558–13564.
44 T. Fukaminato, M. Tanaka, L. Kuroki and M. Irie, Invisible photochromism of diarylethene derivatives, *Chem. Commun.*, 2008, 3924–3926.
45 S. Aloïse, R. Yibin, I. Hamdi, G. Buntinx, A. Perrier, F. Maurel, D. Jacquemin and M. Takeshita, The photochemistry of inverse dithienylethene switches understood, *Phys. Chem. Chem. Phys.*, 2014, **16**, 26762–26768.
46 K. Uchida and M. Irie, A Photochromic Dithienylethene That Turns Yellow by UV Irradiation, *Chem. Lett.*, 1995, 969–970.
47 M. Irie and M. Morimoto, Photoswitchable Turn-on Mode Fluorescent Diarylethenes: Strategies for Controlling the Switching Response, *Bull. Chem. Soc. Jpn.*, 2018, **91**, 237–250.
48 Y. Takagi, T. Kunishi, T. Katayama, Y. Ishibashi, H. Miyasaka, M. Morimoto and M. Irie, Photoswitchable fluorescent diarylethene derivatives with short alkyl chain substituents, *Photochem. Photobiol. Sci.*, 2012, **11**, 1661–1665.
49 D. Kim, J. E. Kwon and S. Y. Park, Fully Reversible Multistate Fluorescence Switching: Organogel System Consisting of Luminescent Cyanostilbene and Turn-On Diarylethene, *Adv. Funct. Mater.*, 2018, **28**, 1706213.
50 D. Okada, Z. Lin, J. Huang, O. Oki, O. Morimoto, X. Liu, T. Minari, S. Ishii, T. Nagao, M. Irie and Y. Yamamoto, Optical microresonator arrays of fluorescence-switchable diarylethenes with unreplicable spectral fingerprints, *Mater. Horiz.*, 2020, **7**, 1801–1808.

51 D. Kim, K. Jeong, J. E. Kwon, H. Park, S. Lee, S. Kim and S. Y. Park, Dual-color fluorescent nanoparticles showing perfect color-specific photoswitching for bioimaging and super-resolution microscopy, *Nat. Commun.*, 2019, **10**, 3089.

52 B. Roubinet, M. L. Bossi, P. Alt, M. Leutenegger, H. Shojaei, S. Schnorrenberg, S. Nizamov, M. Irie, V. N. Belov and S. W. Hell, Carboxylated Photoswitchable Diarylethenes for Biolabeling and Super-Resolution RESOLFT Microscopy, *Angew. Chem., Int. Ed.*, 2016, **55**, 15429–15433.

53 K. Uno, A. Aktalay, M. L. Bossi, M. Irie, V. N. Belov and S. W. Hell, Turn-on mode diarylethenes for bioconjugation and fluorescence microscopy of cellular structures, *Proc. Natl. Acad. Sci. U. S. A.*, 2021, **118**, e2100165118.

54 H. Sotome, D. Kitagawa, T. Nakahama, S. Ito, S. Kobatake, M. Irie and H. Miyasaka, Cyclization reaction dynamics of an inverse type diarylethene derivative as revealed by time-resolved absorption and fluorescence spectroscopies, *Phys. Chem. Chem. Phys.*, 2019, **21**, 8623–8632.

55 K. Uno, M. L. Bossi, V. N. Belov, M. Irie and S. W. Hell, Multicolour fluorescent "sulfide–sulfone" diarylethenes with high photo-fatigue resistance, *Chem. Commun.*, 2020, **56**, 2198–2201.

56 T. Fukaminato, T. Doi, N. Tamaoki, K. Okuno, Y. Ishibashi, H. M. Miyasaka and M. Irie, Single-Molecule Fluorescence Photoswitching of a Diarylethene–Perylenebisimide Dyad: Non-destructive Fluorescence Readout, *J. Am. Chem. Soc.*, 2011, **133**, 4984–4990.

57 M. Berberich, M. Natali, P. Spenst, C. Chiorboli, F. Scandola and F. Würthner, Nondestructive Photoluminescence Read-Out by Intramolecular Electron Transfer in a Perylene Bisimide-Diarylethene Dyad, *Chem. – Eur. J.*, 2012, **18**, 13651–13664.

58 K. Uno, M. L. Bossi, T. Konen, V. N. Belov, M. Irie and S. W. Hell, Asymmetric Diarylethenes with Oxidized 2-Alkylbenzothiophen-3-yl Units: Chemistry, Fluorescence, and Photoswitching, *Adv. Opt. Mater.*, 2019, **7**, 1801746.

59 A. M. Brouwer, Standards for photoluminescence quantum yield measurements in solution (IUPAC Technical Report), *Pure Appl. Chem.*, 2011, **83**, 2213–2228.

60 M. J. Frisch, G. W. Trucks, H. B. Schlegel, G. E. Scuseria, M. A. Robb, J. R. Cheeseman, G. Scalmani, V. Barone, B. Mennucci, G. A. Petersson, H. Nakatsuji, M. Caricato, X. Li, H. P. Hratchian, A. F. Izmaylov, J. Bloino, G. Zheng, J. L. Sonnenberg, M. Hada, M. Ehara, K. Toyota, R. Fukuda, J. Hasegawa, M. Ishida, T. Nakajima, Y. Honda, O. Kitao, H. Nakai, T. Vreven, J. A. Montgomery Jr., J. E. Peralta, F. Ogliaro, M. Bearpark, J. J. Heyd, E. Brothers, K. N. Kudin, V. N. Staroverov, R. Kobayashi, J. Normand, K. Raghavachari, A. Rendell, J. C. Burant, S. S. Iyengar, J. Tomasi, M. Cossi, N. Rega, J. M. Millam, M. Klene, J. E. Knox, J. B. Cross, V. Bakken, C. Adamo, J. Jaramillo, R. Gomperts, R. E. Stratmann, O. Yazyev, A. J. Austin, R. Cammi, C. Pomelli, J. W. Ochterski, R. L. Martin, K. Morokuma, V. G. Zakrzewski, G. A. Voth, P. Salvador, J. J. Dannenberg, S. Dapprich, A. D. Daniels, Ö. Farkas, J. B. Foresman, J. V. Ortiz, J. Cioslowski and D. J. Fox, *Gaussian 09 Revision D.01*, Gaussian Inc., Wallingford, CT, 2009.

61 P. Rodgers, What is a diffraction limit?, *Nat. Nanotechnol.*, 2009, DOI: **10.1038/nnano.2009.115**.

62 S. W. Hell, S. Jakobs and L. Kastrup, Imaging and writing at the nanoscale with focused visible light through saturable optical transitions, *Appl. Phys. A*, 2003, **77**, 859–860.

63 T. L. Andrew, H. Y. Tsai and R. Menon, Confining light to deep subwavelength dimensions to enable optical nanopatterning, *Science*, 2009, **324**, 917–921, DOI: **10.1126/science.1167704**.

64 For the use of spyropyranes (a) and azobenzenes (b, c), see: (*a*) H. Vijayamohanan, E. F. Palermo and C. K. Ullal, Spirothiopyran-Based Reversibly Saturable Photoresist, *Chem. Mater.*, 2017, **29**, 4754–4760; (*b*) Y. Cao, Z. Gan, B. Jia, R. A. Evans and M. Gu, High-photosensitive resin for super-resolution direct-laser-writing based on photoinhibited polymerization, *Opt. Express*, 2011, **19**, 19486–19494; (*c*) H.-Y. Tsai, S. W. Thomas and R. Menon, Parallel scanning-optical nanoscopy with optically confined probes, *Opt. Express*, 2010, **18**, 16014–16024.

65 R. Menon and H. I. Smith, Absorbance-modulation optical lithography, *J. Opt. Soc. Am. A*, 2006, **23**, 2290–2294.